

Queensland University of Technology
Brisbane Australia

This may be the author's version of a work that was submitted/accepted for publication in the following source:

Wickramasinghe, Wasanthi Ramyalatha, Thambiratnam, David, Chan, Tommy, & Nguyen, Andy
(2016)
Vibration characteristics and damage detection in a suspension bridge.
Journal of Sound and Vibration, *375*, pp. 254-274.

This file was downloaded from: https://eprints.qut.edu.au/221110/

© Consult author(s) regarding copyright matters

This work is covered by copyright. Unless the document is being made available under a Creative Commons Licence, you must assume that re-use is limited to personal use and that permission from the copyright owner must be obtained for all other uses. If the document is available under a Creative Commons License (or other specified license) then refer to the Licence for details of permitted re-use. It is a condition of access that users recognise and abide by the legal requirements associated with these rights. If you believe that this work infringes copyright please provide details by email to qut.copyright@qut.edu.au

License: Creative Commons: Attribution-Noncommercial-No Derivative Works 2.5

Notice: *Please note that this document may not be the Version of Record (i.e. published version) of the work. Author manuscript versions (as Submitted for peer review or as Accepted for publication after peer review) can be identified by an absence of publisher branding and/or typeset appearance. If there is any doubt, please refer to the published source.*

https://doi.org/10.1016/j.jsv.2016.04.025

Vibration Characteristics and Damage Detection in a Suspension Bridge

Wasanthi R. Wickramasinghe, David P. Thambiratnam, Tommy H.T. Chan & Theanh Nguyen

*School of Civil Engineering & Built Environment,

Queensland University of Technology (QUT),

Brisbane, Australia.

Abstract

Suspension bridges are flexible and vibration sensitive structures that exhibit complex and multi-modal vibration. Due to this, the usual vibration based methods could face a challenge when used for damage detection in these structures. This paper develops and applies a mode shape component specific damage index (DI) to detect and locate damage in a suspension bridge with pre-tensioned cables. This is important as suspension bridges are large structures and damage in them during their long service lives could easily go un-noticed. The capability of the proposed vibration based DI is demonstrated through its application to detect and locate single and multiple damages with varied locations and severity in the cables of the suspension bridge. The outcome of this research will enhance the safety and performance of these bridges which play an important role in the transport network.

KEYWORDS:

Suspension bridges, Vibration characteristics, Cables, Vibration based damage detection, Modal flexibility, Component specific damage index, Noise

*Corresponding author e-mail: d.thambiratnam@qut.edu.au; Tel: 61 7 3138 1467; Fax: 61 7 3138 1170

1. Introduction

As transport infrastructure systems, particularly bridges, in many countries are rapidly aging, structural deterioration can set in. Environmental influences, changes in load characteristics and random actions [1] accelerate the structural deterioration and can cause damage leading to expensive retrofitting or bridge failure. The importance of detecting damage in these bridges at an early stage and carrying out the necessary retrofitting to prevent bridge failure is therefore obvious.

Structural Health Monitoring (SHM) has emerged as an approach that can address this need. Current SHM systems are integrated with a variety of damage detection methods, which are global and local in nature. Limitations in local methods necessitate the non-destructive and global techniques for damage diagnosis. This has led to continuous development in vibration based damage detection (VBDD) methods in SHM systems. The basic principle of vibration based SHM is that the damage in a structure changes its structural properties which in turn results in changes in its vibration characteristics. A change in the vibration characteristics can hence be used to detect damage in a structure. In the context of VBDD technology, methods that use Damage Indices (DIs) are effective, inexpensive and have the ability to automate the damage assessment process [2, 3]. Many researchers have used Damage Index (DI) methods to successfully detect and locate damage in structures constructed with different material such as steel [4, 5], composites [6] reinforced concrete [3] and timber [7]. In the literature, different vibration characteristics such as natural frequencies [8, 9], damping ratios [10, 11], mode shapes [12, 13], derivatives of mode shapes [4, 14, 15], modal flexibility [7, 16-23] and modal strain energy values [3, 24-26] have been used to developed the DIs for damage detection in various structures. A special DI based on Poincare´ maps (which contain data for the displacements and the velocities of the structure) was proposed by Manoach and Trendafilova [27] to identify damage in rectangular plates.

Suspension bridges are increasingly used in today's infrastructure system to span large distances and are rich in architectural features and aesthetical aspects. They are large structures and their main cables may be subjected to severe corrosion and fatigue damage, which can go unnoticed. These bridges are flexible structures with low stiffness and low mass. They are vibration sensitive and exhibit complex vibration characteristics. Such vibration is multi-modal and coupled and hence it is difficult to identify the damage sensitive modes for use with the normal vibration based methods for detecting damage. Due to this reason the use of vibration based DI to assess damage in suspension bridge cables has been limited.

Among different VBDD techniques the traditional modal flexibility (MF) method is a promising method which incorporates the natural frequencies and mass normalized mode shapes. It usually requires a few of the lower order modes for detecting damage in structures and has been used by a number of researchers for locating damage in beam and plate like structures [16-18, 26, 28]. Wang et al. [19] identified that MF was a sensitive damage indicator compared with other modal indices in detecting damage in the bearings, decks and

hangers of the Tsing Ma Bridge. Choi et al. [7] also used the changes in flexibility to develop a new hybrid algorithm to estimate damage severity in timber structures. Relative flexibility change (RFC) between intact and damaged states of the cable stayed bridge was studied by Ni et al. [20], whose RFC index was successful in locating damage in single damage scenarios in the absence of ambient effects. However difficulties were encountered in detecting and locating damage in cross girders. Moragaspitiya et al. [21] predicted the axial shortening of vertical load bearing elements of reinforced concrete buildings using the MF method. Montazer and Seyedpoor [22] developed a new damage index named as strain change based on flexibility index (SCBFI) which was used for locating multiple damage cases in truss systems and demonstrated its capability. Recently, Sung et al. [23] developed a method based on MF to detect damage in cantilever beam type structures. It was successfully applied to identify damage in a ten story building by both numerically and experimentally for single and multiple damage cases. The literature confirms that the MF method has a wide variety of applications in damage diagnosis studies but not in detecting and locating damage in the main cables of suspension bridges.

This paper develops and applies a mode shape component specific damage index (DI) that can successfully detect and locate damage in the main cables of a suspension bridge with pre-tensioned cables. These are very important components of a suspension bridge. This special VBDD method is a modified form of the traditional MF method and incorporates only a few lower order modes and their components. It is able to overcome the issues associated with the complex vibration exhibited by suspension bridges and is easy to calculate and apply. The effectiveness of the proposed DI is demonstrated under a range of damage scenarios.

To illustrate the proposed method a laboratory model of a suspension bridge with three sets of cables namely; top supporting cables (TSC), pre-tensioned reverse profiled (bottom) cables (RPC) in the vertical plane and pre-tensioned bi-concave side cables (BCSC) in the horizontal plane is considered. These cables serve different structural actions in the bridge. A FE model of this bridge was developed and validated using vibration data from the laboratory performed experiments. This was then used to examine the competency of the component specific DI under different damage scenarios involving single and multiple damages and varying damage intensities in the different cables of this rather complex bridge structure. It is shown that the proposed DI provides better and more reliable results compared to those from the traditional MF method. This paper illustrates the application of the

proposed DI to a three dimensional suspension bridge model which exhibits complex vibration characteristics. Other case studies related to real suspension bridges are presented in reference [29]. The research outcomes will enable the timely retrofitting of cables to ensure the safe operation of suspension bridges in the infrastructure and optimal allocation of public resources for retrofitting and maintenance.

2. Vibration Based Component Specific Damage Indices

The MF method is a widely accepted technique in damage detection which associates vibration characteristics of a structure that include natural frequencies and mass normalized mode shapes. MF of a structure converges rapidly with increasing frequency and can be therefore computed using only a few lower order modes [16]. It does not require any analytical model of a structure to evaluate the flexibility and can be used with only the experimental data collected from the structure (data from experimental modal analysis (EMA) can be used directly in computing MF). However, online monitoring systems instrumented in large scale structures can only measure ambient vibration response which means mass normalized mode shape data is not available. In order to apply the MF method in large scale structures, many researchers [30-33] developed various methods to calculate the MF with ambient vibration measurements with and without use of FEM. The MF method is widely used in SHM application due to its accuracy, convenient computation and ease of application [21]. The MF, F_x at a location x of a structure can be written as;

$$F_x = \sum_{i=1}^{m} \frac{1}{\omega_i^2} \phi_{xi} \phi_{xi}^T \tag{1}$$

Where i ($i=1, 2, 3 \ldots m$) is the mode number considered and ϕ_{xi} is the value of the i^{th} mode shape at x. In complex structures measured modes are less than the analytical modes available, with only a limited number of lower order modes being measured practically [20]. In the above Eq., m and ω_i are the total number of modes considered and the natural frequency of the structure at mode i, respectively.

When a structure is subjected to damage or deterioration, its stiffness is reduced and the flexibility is increased. This modifies its vibration characteristics. The resulting modal flexibilities of the structure are represented in Eqs. 2 and 3 respectively at the damaged and undamaged states of the structure.

$$F_{xD} = \left[\sum_{i=1}^{m} \frac{1}{\omega_i^2} \phi_{xi} \phi_{xi}^T \right]_D \tag{2}$$

$$F_{xH} = \left[\sum_{i=1}^{m} \frac{1}{\omega_i^2} \phi_{xi} \phi_{xi}^T\right]_H \tag{3}$$

Here, subscripts *D* and *H* denote the damaged and undamaged (healthy) states of the structure respectively. Eq. 4 below captures the change in MF of the structure due to damage. In order to determine the MF at undamaged and damaged states, sensors attached to the suspension bridges can be used to collect the acceleration data and calculate ω_i and ϕ_{xi} (vibration properties) by modal analysis methods such as Data Driven Stochastic Subspace Identification (SSI-DATA) (described in section 3.4). In measuring vibration properties, the first state where the vibration properties are measured defines the baseline (healthy) state, whereas all subsequent measurements correspond to the damaged state.

$$F_{xD} - F_{xH} = \left[\sum_{i=1}^{m} \frac{1}{\omega_i^2} \phi_{xi} \phi_{xi}^T\right]_D - \left[\sum_{i=1}^{m} \frac{1}{\omega_i^2} \phi_{xi} \phi_{xi}^T\right]_H \tag{4}$$

In this study, F_{xD} - F_{xH} is normalized by the F_{xH} and hence the damage index for locating damage in a structure is written as in Eq. 5. The normalized damage index (defined below) determines the relative change of modal flexibility, which detects the damage quite accurately.

$$DI = \frac{\left[\sum_{i=1}^{m} \frac{1}{\omega_i^2} \phi_{xi} \phi_{xi}^T\right]_D - \left[\sum_{i=1}^{m} \frac{1}{\omega_i^2} \phi_{xi} \phi_{xi}^T\right]_H}{\left[\sum_{i=1}^{m} \frac{1}{\omega_i^2} \phi_{xi} \phi_{xi}^T\right]_H} \tag{5}$$

In general, suspension bridges can vibrate with lateral, vertical, torsional and coupled modes [34]. It is very difficult to identify damage sensitive modes in a suspension bridge and in particular to measure the rotational coordinates of torsional and coupled modes practically. Most damage detection methods therefore, incorporate mode shapes that include translational coordinates. Further, as the significant mode shape components can be measured in the lateral and vertical directions, this paper defines and tests two corresponding damage indices. One index is based on the structure's vertical components of mode shapes and the other is based on its lateral components of mode shapes. Eq. 5 is hence rewritten as Eqs. 6 and 7 to accommodate the proposed component specific *DIs*, where the subscripts *V* and *L* denote the vertical and lateral components of mode shapes, respectively. Component specific DIs based on modal flexibility have not been treated in the literature, but Li, Yang and Hu [35] have proposed the consideration of mode shape components for modal strain energy.

$$DI_V = \frac{\left[\sum_{i=1}^{m} \frac{1}{\omega_i^2} \phi_{xi} \phi_{xi}^T\right]_{DV} - \left[\sum_{i=1}^{m} \frac{1}{\omega_i^2} \phi_{xi} \phi_{xi}^T\right]_{HV}}{\left[\sum_{i=1}^{m} \frac{1}{\omega_i^2} \phi_{xi} \phi_{xi}^T\right]_{HV}} \quad (6)$$

$$DI_L = \frac{\left[\sum_{i=1}^{m} \frac{1}{\omega_i^2} \phi_{xi} \phi_{xi}^T\right]_{DL} - \left[\sum_{i=1}^{m} \frac{1}{\omega_i^2} \phi_{xi} \phi_{xi}^T\right]_{HL}}{\left[\sum_{i=1}^{m} \frac{1}{\omega_i^2} \phi_{xi} \phi_{xi}^T\right]_{HL}} \quad (7)$$

Since damage alters the stiffness of the structure and increases its flexibility, theoretically, peaks should appear in the damage index curves defined in Eqs. 6 and 7 corresponding to the damage location. However, each vibration mode in the suspension bridge has components in the lateral and vertical directions. The mass participating in each direction (mass participation factor) varies for the different vibration modes in the suspension bridge. The mode shape component with a higher mass participation will contribute towards the prediction of damage more accurately. It is hence worthwhile to study the competency of the DIs based on the vertical and lateral components of the different modes for detecting and locating damage in suspension bridges.

This paper compares the performance of the proposed component specific DIs (defined in Eqs. 6 and. 7 above) with that of the (component specific) MF difference (defined in Eqs. 8 and 9) based on the originally developed MF method by Pandey and Biswas [16, 18]. In this study, MF difference is also calculated using both vertical and lateral components of mode shapes as shown in Eqs. 8 and 9 respectively. These equations were obtained by rewriting Eq. 4 for the two specific components of the mode shapes considered herein.

$$MFD_V = \left[\sum_{i=1}^{m} \frac{1}{\omega_i^2} \phi_{xi} \phi_{xi}^T\right]_{DV} - \left[\sum_{i=1}^{m} \frac{1}{\omega_i^2} \phi_{xi} \phi_{xi}^T\right]_{HV} \quad (8)$$

$$MFD_L = \left[\sum_{i=1}^{m} \frac{1}{\omega_i^2} \phi_{xi} \phi_{xi}^T\right]_{DL} - \left[\sum_{i=1}^{m} \frac{1}{\omega_i^2} \phi_{xi} \phi_{xi}^T\right]_{HL} \quad (9)$$

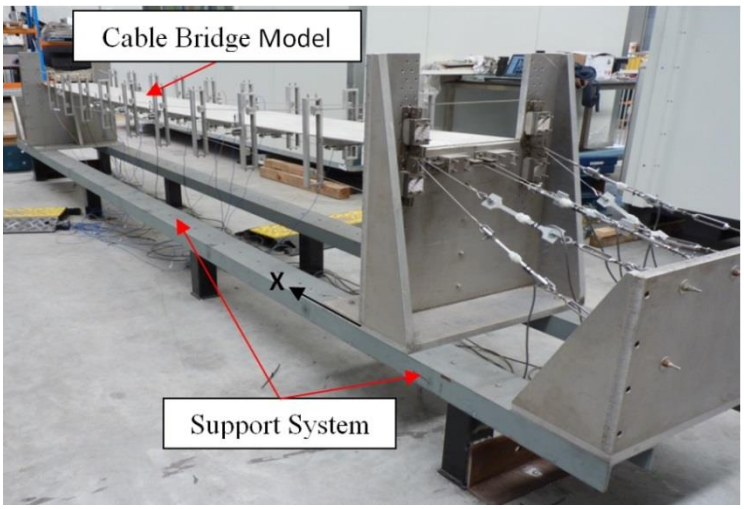
3. Experimental Testing of the Suspension Bridge Model

FE modelling is extensively used in damage detection studies due to the difficulty of applying a physical damage to real structures. In this paper, therefore, a validated FE model using the results of self-performed experiments on the laboratory suspension bridge model was used to simulate various damage scenarios. It was then used to obtain the vibration properties in both the damaged and undamaged states and thereby to verify the proposed

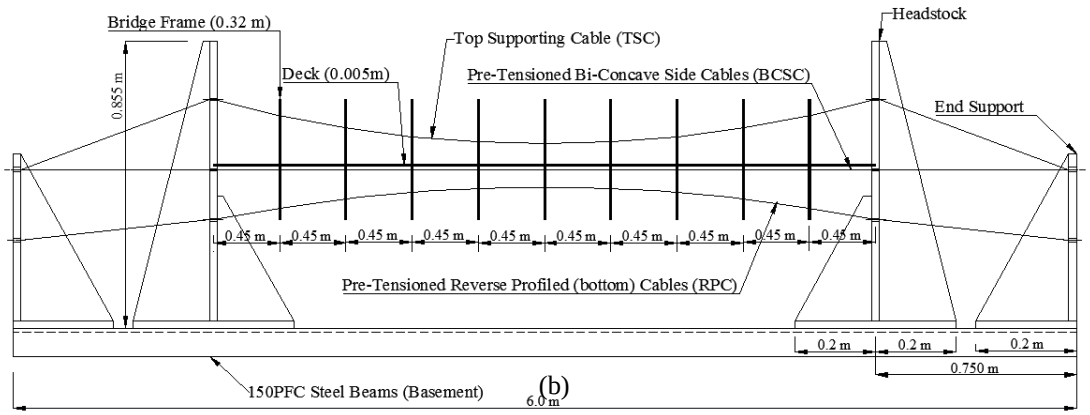
damage detection methodology. Two different tests were conducted on the laboratory model, namely; static and vibration tests which were used to obtain static and dynamic behaviours respectively.

3.1 Laboratory suspension bridge model for vibration testing

The laboratory suspension bridge model used in this study was designed and constructed in the Structures Laboratory at Queensland University of Technology. It consists of two components: namely, cable bridge model and support system (as shown in Fig. 1). In this paper, the cable bridge model is the main focus and its vibration parameters are the major concern in experimental testing. The support system provides anchorage to the cable bridge model.



(a)



(b)

Fig. 1. (a) The laboratory suspension bridge model (b) Schematic diagram of the laboratory suspension bridge model

The cable bridge model consists of a cable system, transverse bridge frames and deck units. It spans of 4.5 m and the cable system comprises of three cable clusters: TSCs, pre-tensioned RPCs (bottom) in the vertical plane and pre-tensioned BCSCs in the horizontal plane. Stainless steel wire strands (7x19) of 3.2mm and 1.6mm nominal diameter are used for the TSCs and both pre-tensioned RPCs (bottom) in the vertical plane and the BCSCs in the horizontal plane respectively. The two parallel TSCs have catenary profiles which provide tension forces to support weight of the bridge, applied loads and internal forces induced by the pre-tensioned bottom cables. The role of the two parallel pre-tensioned RPCs in the vertical plane is to introduce pre-tension forces and provide internal vertical forces to the transverse bridge frames and the top supporting cables. The main structural function of the pair of pre-tensioned BCSCs in the horizontal plane is to provide horizontal stiffness to the cable bridge model. When the pre-tensioned bottom and/or side cables are slack, they carry small tension forces to support only their own weights and they cannot resist any external loads or cannot contribute to the stiffness of the structure. However, small tension forces in these cables can provide sufficient restraining forces to prevent the transverse frames from swaying in the lateral direction.

Nine transverse bridge frames at 450mm from each other are hung from the TSCs, and further restrained by the pre-tensioned RPCs in the vertical plane and the pre-tensioned BCSCs in the horizontal plane. The main function of the transverse bridge frames is to support the deck and hold the cables in the desired profiles. These frames comprise of a cross member (to support the deck), side members, end caps, and cable plugs (to hold cables in the required profiles). Transverse bridge frames have in plane stiffness to protect against collapse under in plane forces, but they contribute little to the longitudinal, lateral and rotational stiffness of the system.

In each bridge frame, there are six cable plugs to hold the cables in the required cable profiles. TSCs and pre-tensioned RPCs in the vertical plane are supported by the cable plugs arranged at the two sides of the bridge frame. These cable plugs can be adjusted along the sockets in the transverse frame’s side members by turning of the thread rods. Additional two cable plugs are arranged under the cross member of the bridge frame to hold the BCSCs in the horizontal plane. In each span, eight deck segments are supported on the cross member of the transverse bridge frames. The bridge deck units and main parts of the transverse bridge frames are made of aluminium, except thread rods which are made of stainless steel.

Anchorage to the cable bridge is provided by the support system. It encompasses headstocks, cable clamps, load cells, turnbuckles, end supports and basements. The two aluminium headstocks of the support system can provide the required support to the cables to suit the different cable configurations. The details of the support system are illustrated in Fig. 2.

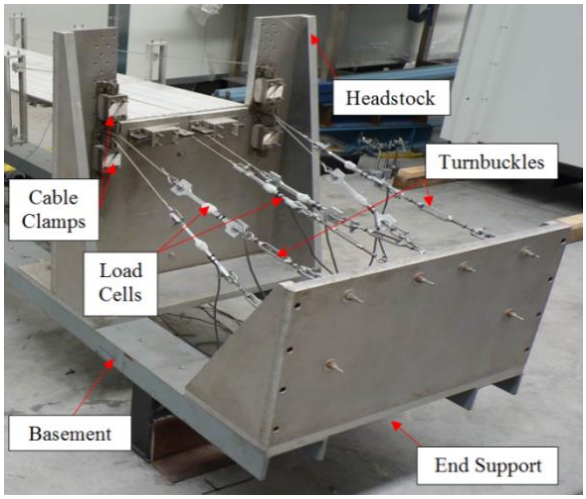


Fig. 2. The support system

Twelve aluminium specimens with two transducer specific strain gauges mounted on either side are used to measure the tension forces in the cables and are called load cells (Fig. 2). In order to measure these tension forces, load cells were connected to an Electronic Data Acquisition System (eDAQ).

3.2 Experimental vibration testing

Once the calibration of load cells was completed, two experimental tests: static and vibration tests were conducted. Two bridge model cases were considered to investigate the static and dynamic behaviour of the bridge. In case 1, the bridge model was designed to have cable configuration with only TSCs and bottom pre-tensioned RPCs (in the vertical plane) with the desired tension forces of 1400N and 300N respectively. In case 2, the bridge model was designed to have all the pre-tensioned cables including TSCs, bottom pre-tensioned RPCs and pre-tensioned BCSCs with the desired tension forces of 1400N, 400N and 300N respectively. Due to the sensitivity of the load cells, results will be presented for average values of the tension force during testing. A preliminary FE model was developed to approximately identify the static and dynamic behaviour of the bridge before conducting experiments. The experimental process including both static and vibration tests are shown in Fig. 3.

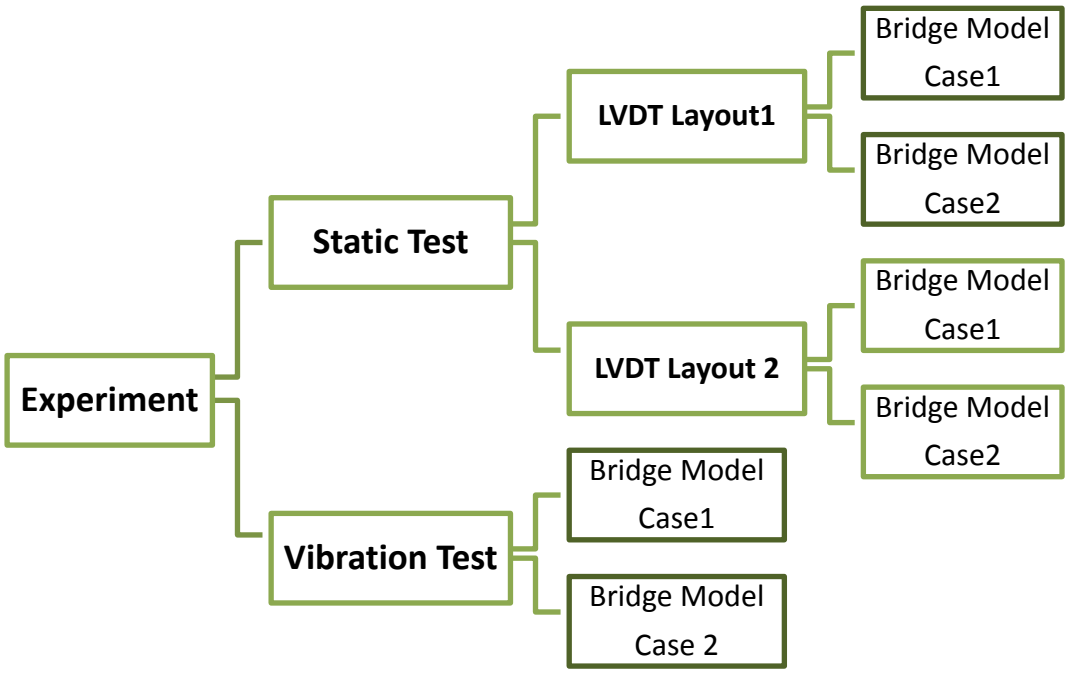


Fig. 3. The experiment process

3.3 Static test

As a precursor to the vibration test, the static test was conducted to obtain the static behaviour of the cable bridge when subjected to static loading. Test results were used to verify the bridge geometry (symmetricity). Results from the static test are not presented herein as the focus of this paper pertains to damage detection using the vibration properties of the bridge model and for want of space,

3.4 Vibration test

The use of experiments to obtain the dynamic response of civil structures is a well-established practice, which can be dated back to the mid twentieth century [36]. Input-Output Modal Analysis (also known as EMA) is the traditional method of obtaining the dynamic parameters of a structure basically by measurements of the excitation and the vibration response. Even though it has been applied in different fields, applications of this technique are challenging in large structures due to their lower frequency range and complexities in excitation. Therefore, Output Only Modal Analysis (OMA) (also known as Operational Modal Analysis) has recently gained the attention of the Engineering community. OMA is an experimental procedure to estimate the modal parameters of a structure from measurements of the vibration response only.

Two main groups of OMA methods can be identified; as frequency domain methods and time domain methods. A variety of methods in both frequency and time domains can be

classified under OMA [37]. Among these methods, Data Driven Stochastic Subspace Identification (SSI-DATA) has been identified as the well-known robust time domain method in the OMA family. It can take into account furious modes from measurement noise, avoid spectrum leakage and cope well with dense and closely spaced modes [38-40]. SSI-DATA method relies on directly fitting parametric state space models to the measured responses of a linear and time invariant physical system [40]. Among different estimation algorithms for SSI-DATA (Structural Vibration Solutions A/S. 2011), Un-weighted Principal Component (UPC) has been most commonly used in OMA of civil structure. In this experiment, modal parameters were extracted by the SSI-DATA (UPC) in ARTeMIS modal analysis software. The instrument setup used in the experiment, testing procedure and vibration test results are discussed briefly in the next few sections.

3.4.1 Instrument setup

Prior to vibration testing, the data acquisition system was established; which encompassed 15 single-axial PCB® 393B05 integrated circuit piezoelectric accelerometers, positioned to measure vertical and lateral accelerations. These accelerometers were attached to each of the five bridge frames. Layout of accelerometers is illustrated in Fig. 4. In each frame, two accelerometers measured the accelerations in the vertical direction and the third measured the accelerations in the lateral direction. Additionally, dummy accelerometers (Fig. 5) were installed in the lateral direction at the five bridge frames to simulate identical point mass loading on both sides of the bridge frame. The data acquisition system was operated by a National Instruments (NI) data acquisition system including NI cDAQ 9172 chassis, NI 9234 dynamic signal acquisition modules and LabVIEW signal Express software.

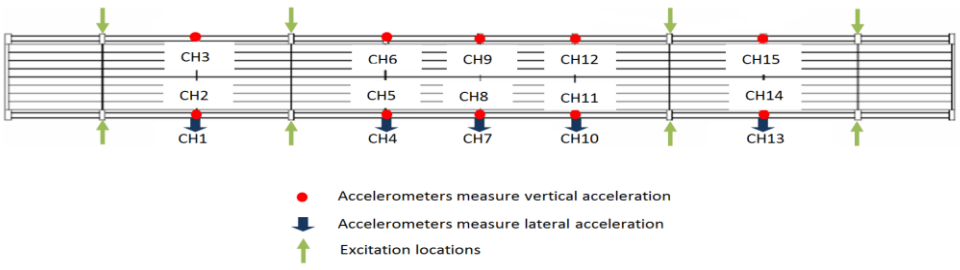


Fig. 4. Accelerometer layout and excitation locations in the plan view of bridge deck

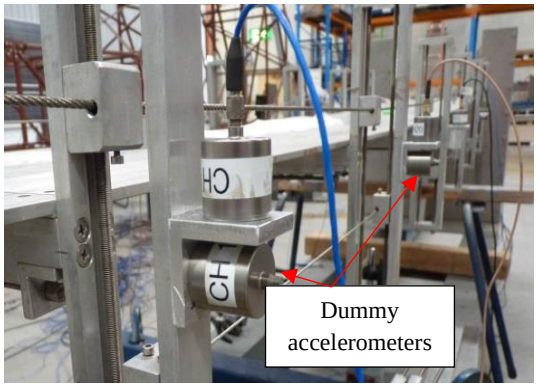


Fig. 5. Dummy accelerometers

3.4.2 Vibration testing procedure

Before vibration testing commenced, it was necessary to determine two parameters. The first parameter is the length of time series to record the vibration data. It is necessary to ensure that the length of time series is adequate to cover complete or near complete behaviour of the structure under ambient vibration. The total length of time series should be in the range [41] of $T_{min} = \frac{1000\sim2000}{f_{min}}$ sec, where f_{min} is the expected lowest natural frequency measured in Hz. According to the preliminary FE modal analysis, f_{min} is 3.5Hz. Therefore T_{min} is 9.5 minutes (T_{min}=2000/3.5=571.4sec). It was hence necessary to choose the minimum recording time length to be longer than 9.5 minutes. In the vibration test, the recording time was selected as 10 minutes.

The second parameter to consider is the sampling rate of measurements. Commercial software package such as ATReMIS modal analysis software recommends the sampling frequency to be at least f_s=3f_{max}, where f_{max} is the highest natural frequency of interest. In this way, the Nyquist frequency will be at least 1.5 times f_{max} providing some room for avoiding aliasing. The selected sampling rate herein was 2.56 kHz which is a relatively higher value.

Since the bridge model was located in the laboratory and not subjected to any ambient loading, artificial excitation was adopted. In an effort to excite the structure, two researchers provided random tapping for ten minutes and through a foam (to reduce the negative impact as the bridge model is very flexible) with respect to both time and space, at alternating frames. As random excitation is desired in OMA with respect to time, force magnitude needs to be varied while conducting the test. But the magnitude of the applied excitation force was controlled to ensure the excitation signal was within the range of the accelerometers. In order to fulfil the second requirement of OMA (random excitation in space), excitation locations were changed during testing. Fig 4 shows the excitation locations.

Before conducting any tests, the twelve load cells were checked carefully and the turnbuckles attached to the cables were adjusted to obtain the required tension forces. Load cell readings were automatically recorded by eDAQ while conducting the experiments to check any tension losses during testing. All the acceleration data was captured in the time domain and was transferred to the ARTeMIS modal analysis software to obtain the modal parameters.

3.4.3 Vibration test results

The natural frequencies and mode shapes were determined by SSI-DATA (UPC) in ARTeMIS modal analysis software. Two bridge model cases were considered in the vibration tests. In bridge model case1, TSCs and pre-tensioned RPCs were setup to average tension values of 1446N and 326N respectively. In bridge model case2, TSCs, pre-tensioned RPCs and pre-tensioned BCSCs were set up to average tension values of 1403N, 485N and 270N respectively. In each bridge model case only the first five modes were obtained in the experiment for the damage detection studies. Two sets of vibration test results were obtained from the two different bridge models, to enhance the validation of the FE models. The natural frequencies for the bridge model cases1 and 2 (Table 3 and Table 4) and the graphical representation of the mode shapes will be presented and compared with the corresponding numerical results in the next section on FE model validation.

4 Validation of the FE Model of the Laboratory Bridge Structure

The numerical model was developed to represent the actual laboratory structure as close as possible. It was hence necessary to replicate all the geometric features of this complex structure precisely. To achieve this, the commercial finite element analysis software package ANSYS Workbench [42] which is facilitated with graphical user interface for developing complex models as multibody parts, was used.

4.1 Geometry of the laboratory bridge structure

The geometry of the laboratory bridge structure was modelled in the DesignModeler module of ANSYS Workbench. It was modelled as a three dimensional FE model with three parts namely; bridge (nine transverse bridge frames and cables), deck and end supports. As mentioned before, all the bridge members were aluminium except the thread rods and cables which were stainless steel. Member sizes used for the FE modelling of the laboratory bridge structure are presented in Table 1 and the corresponding material characteristics are given in Table 2.

Table 1 Cross section dimension of the bridge elements

Member	Cross Section Dimension (mm)
End Cap	60 x 25 x 10
Side Member	300 x 25 x 10
Cross Member	400 x 25 x 30
Deck Unit	450 x 48 x 5
Thread road	5mm diameter
Top supporting cables	3.2mm 7x19 strand
Pre-tensioned reverse profiled (bottom) cables in vertical plane	1.6mm 7x19 strand
Pre-tensioned bi-concave side cables in the horizontal plane	1.6mm 7x19 strand

Table 2 Material characteristics

Material	Density (kg/m^3)	Young's Modulus E (N/m^2)	Poisson's Ratio ν
Aluminium	2745	6.700E+10	0.33
Stainless Steel	7850	2.000E+11	0.25
3.2mm - 7x19 Stainless steel wire	5679	4.725E+10	0.30
1.6mm - 7x19 Stainless steel wire	4765	4.688E+10	0.30
Aluminium-Deck	3026	6.900E+10	0.33

4.2 Vibration analysis of laboratory bridge structure

Geometry of the cable bridge was created in the DesignModeler module and transferred into the Mechanical module of the ANSYS Workbench for analysis. In the Mechanical module, correct material characteristics were assigned to each element of the bridge and point masses each of 0.132Kg (weight of accelerometers + weight of aluminium equal angle) were added to the bridge frames at the locations where accelerometers were attached. Since the accelerometers were attached to the bridge while carrying out vibration testing, these point masses were added to the FE model for the vibration analysis.

All the elements of the bridge were modelled as beam and link elements except the end supports. BEAM188 element type was used to simulate bridge frames and deck elements, while the end supports were modelled using SHELL181 element type. All cables associated in this bridge model were very thin cables having very small bending stiffness. Therefore these cables were simulated by LINK180 element with tension only option.

In the FE model, connectivity of the cables and cable plugs in bridge frames were modelled as rigid connections as there was no allowance for the cables to rotate or displace at those locations in the cable bridge model. In the nine transverse bridge frames, all the members were considered as rigidly connected together at the intersection locations.

A Pre-stressed Modal Analysis was conducted to obtain the natural frequencies and mode shapes of the bridge FE model. Towards this end, initially, a nonlinear static analysis with large deflection option was conducted to obtain the stress stiffening matrix caused by the internal forces due to the dead loads acting on the bridge. Later, the modal analysis was performed on the basis of the deformed equilibrium configuration of the bridge to obtain the natural frequencies and mode shapes.

In the experiments, vibration tests were conducted for the two bridge model cases. FE models for each test case were developed and a comparison of results with those obtained experimentally is presented in the next section.

4.3 Vibration test data and validation of the FE model

To validate the FE model, a comparison of experimental and FE model results was made. The tension forces of cables, natural frequencies and mode shapes obtained from the FE analysis were compared with those from the vibration tests. To achieve the validation of the FE model in this study, model updating was done manually to modify the structural parameters of the FE model such that the difference in the natural frequencies obtained FE model and from the experiment are minimised. With the change of structural parameters such as cable tension, connectivity of structural elements, support conditions and member offsets, the initial FE model was updated. Validation results are presented in the next section.

The comparison of the tension forces of the cables and natural frequencies of the bridge obtained from FE analysis and experiment was conducted by calculating relative errors:

$T_{error} = \frac{(T_{exp} - T_{fem})}{T_{exp}} \times 100$ and $f_{error} = \frac{(f_{exp} - f_{fem})}{f_{exp}} \times 100$ respectively.

In the above expressions $T_{\exp}$ and f_{exp} are tension force and natural frequency obtained in the experiment and T_{fem} and f_{fem} are those obtained in the FE analysis. In addition, mode shapes are also compared. Tables 3 and 4 present the tension forces and first five natural frequencies obtained from the experiment and the FE model. It can be observed that the difference between the experimental and FE results is less than 9% which demonstrates a very good

correlation of results. Mode shapes were also compared for further verification of the vibration analysis and the results are illustrated in Figs. 6 and 7. From the outcomes of the above comparisons, it can be concluded that the FE model is a good representation of the laboratory bridge model and hence the FE modelling techniques were verified. The validated FE model then provides the base line model for vibration based damage detection applications which will be described in the next section.

Table 3 Tension forces and frequencies of bridge model case 1

Element	Tension Force (N)		T_{error} (%)
	T_{exp}	T_{fem}	
Top Cable N	1446	1442	0.28
Bottom Cable N	326	299	8.28
Bottom Horizontal cable N	-	-	-
Mode	**Frequency (Hz)**		f_{error} (%)
	f_{exp}	f_{fem}	
1st Bending - Symmetric	3.714	3.609	2.8
2nd Bending - Anti-symmetric	5.875	5.562	5.3
1st Torsion	5.970	5.703	4.5
3rd Bending - Symmetric	8.369	8.777	-4.9
2nd Torsion	10.407	10.731	-3.1

Table 4 Tension forces and frequencies of bridge model case 2

Element	Tension Force (N)		T_{error} (%)
	T_{exp}	T_{fem}	
Top Cable N	1403	1450	-3.35
Bottom Cable N	485	476	1.86
Bottom Horizontal cable N	270	261	3.33
Mode	**Frequency (Hz)**		f_{error} (%)
	f_{exp}	f_{fem}	
1st Bending - Symmetric	3.791	3.736	1.5
2nd Bending - Anti-symmetric	6.094	5.793	4.9
1st Torsion	6.077	6.001	1.3
3rd Bending - Symmetric	8.719	9.423	-8.1
2nd Torsion	10.625	10.906	-2.6

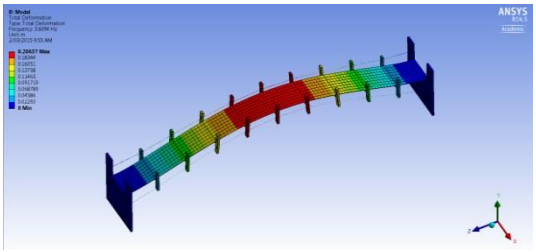
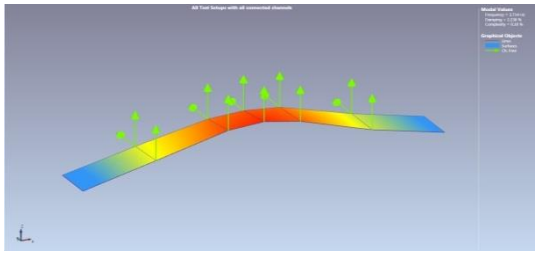
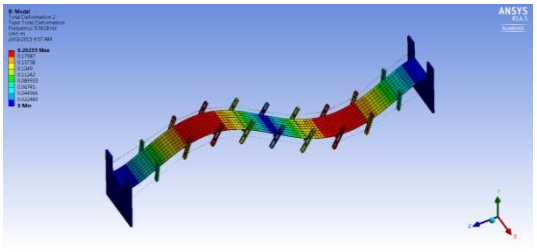
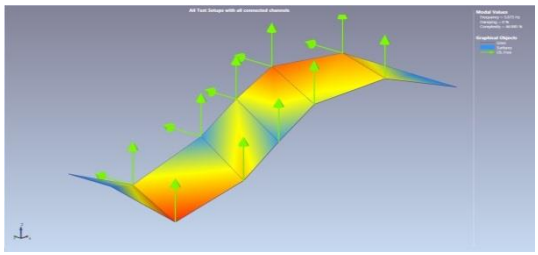
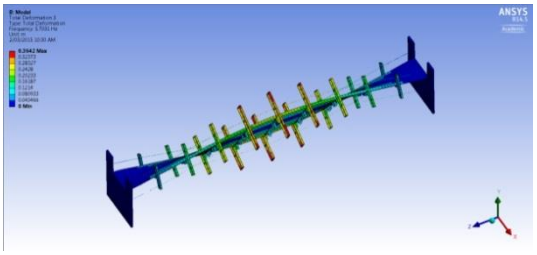
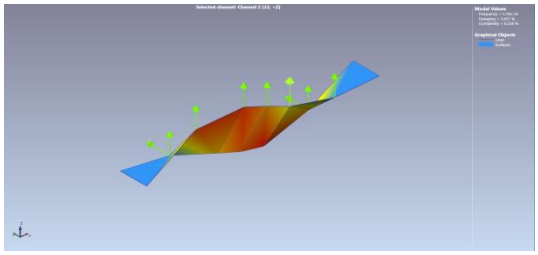
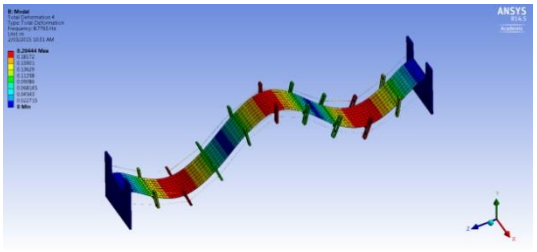
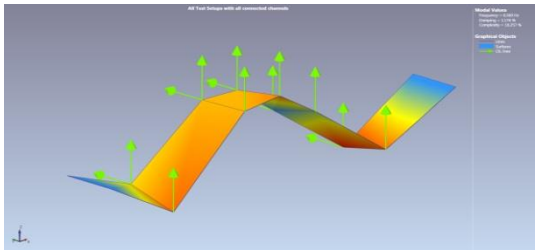
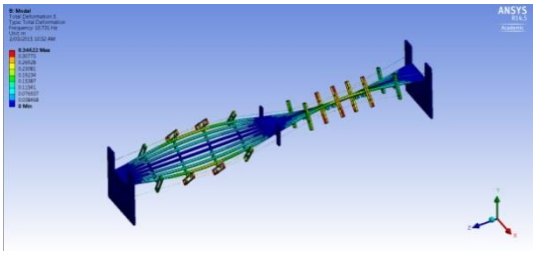
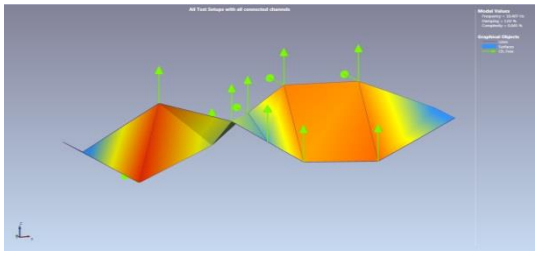
Mode	FEM	Experiment
1st Mode		
2nd Mode		
3rd Mode		
4th Mode		
5th Mode		

Fig. 6. Comparison of mode shapes - bridge model case 1

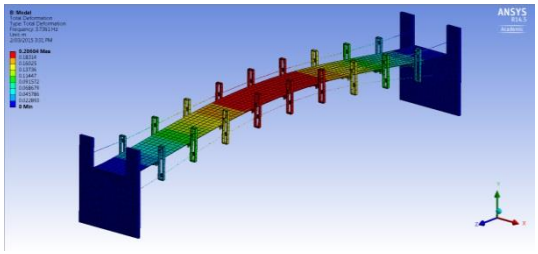
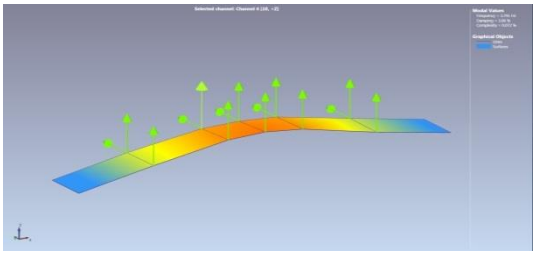
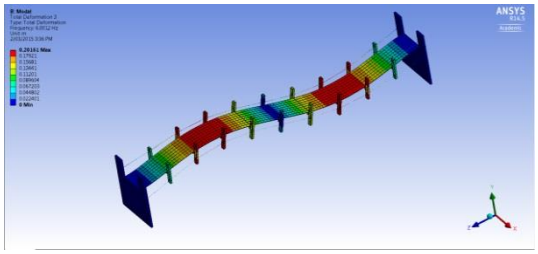
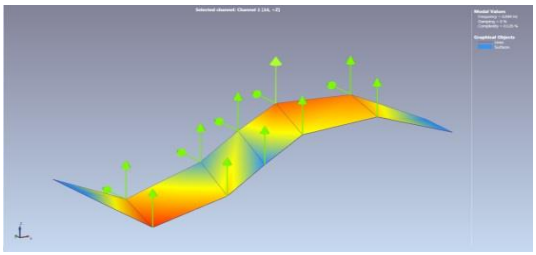
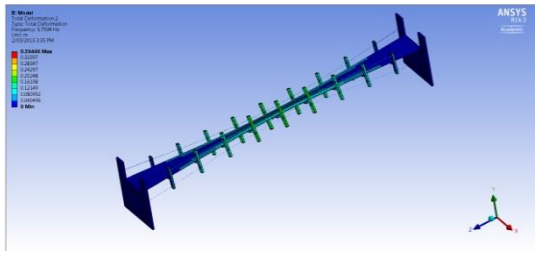
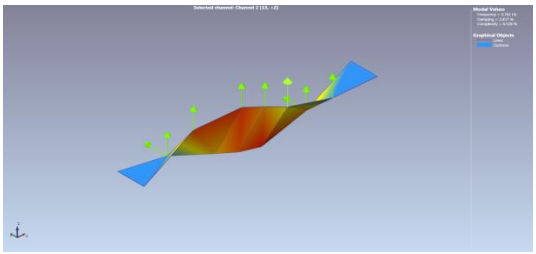
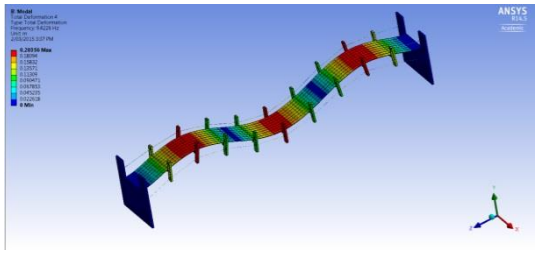
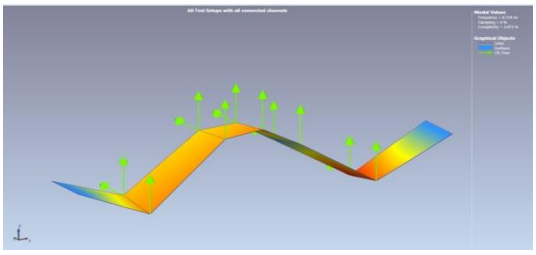
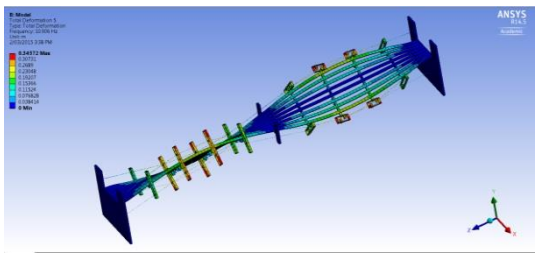
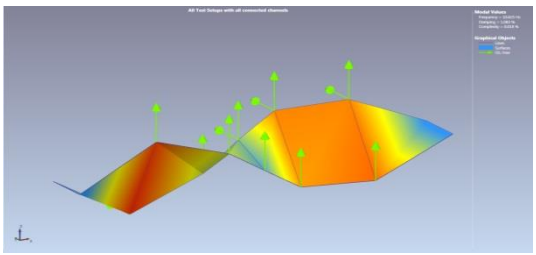
Mode	FEM	Experiment
1st Mode		
2nd Mode		
3rd Mode		
4th Mode		
5th Mode		

Fig. 7. Comparison of mode shapes - bridge model case 2

5 Damage Detection in Cables using Vibration Based Damage Indices

In this study the main objective is to evaluate the competency of the component specific DIs to detect damage in the three different types of cables which play different roles in the bridge. The FE model validated in the previous section of this paper is considered as the undamaged baseline model for VBDD application. Ten damage cases were introduced in the FE model to synthesize the various damage scenarios. It includes two different damage scenarios namely; single damage scenarios and multiple damage scenarios in cables. This study was based on numerical simulation data, and therefore closely spaced mode shape data was used to plot the damage index curves. However, in real practice limited numbers of sensors are used to measure the acceleration data, and hence mode shape reconstruction techniques such as cubic spline interpolation can be used to refine the mode shapes [7].

The results obtained from the proposed DIs are compared with those from the traditional MF method to demonstrate the superior performance of the proposed DIs. The two proposed DIs called the vertical damage index and lateral damage index (defined in section 2) were calculated by using the vertical and lateral components of the first five mode shapes respectively. Similarly, the MF difference vertical and MF difference lateral were also calculated using the vertical and lateral components of the first five mode shapes respectively. Following abbreviations are used in the presentation of the results.

DI_V Damage Index Vertical - calculated by using the vertical components of mode shapes

DI_L Damage Index Lateral - calculated by using the lateral components of mode shapes

MFD_V MF Difference Vertical - calculated by using the vertical components of mode shapes

MFD_L MF Difference Lateral - calculated by using the lateral components of mode shapes

There were three sets of cables (TSC, RPC and BCSC) in the suspension bridge and the two cables in each set are named using subscripts 1 and 2 which refer to cable 1 and cable 2. For example, TSC1 refers to top supporting cable1.

5.1 Damage Scenarios

Damage in FE models can be simulated by changing the Young's modulus or changing the cross section area or removing elements at damage location. This study simulated damage in the cables by reducing Young's modulus of the specified elements. Table 5 below presents

the details of the damage cases considered in this study. In this Table, X is measured along the span of the bridge starting from the right hand end support (Fig. 1).

Table 5 Damage scenarios

Damage Case	Location	Severity of Damage
	Single Damage Scenario	
DC 1	Damage at middle of TSC1 (X=2.250m to X=2.475m)	20%
DC 2	Damage at quarter of TSC 1 (X=1.125m to X=1.350m)	20%
DC 3	Damage at corner of TSC 2 (X=4.275m to X=4.500m)	20%
DC 4	Damage at quarter of RPC1 (X=0.900m to X=1.350m)	20%
DC 5	Damage at corner of RPC1 (X=4.275m to X=4.500m)	20%
DC 6	Damage at middle of BCSC1 (X=2.025 to X=2.475)	20%
DC 7	Damage at corner of BCSC1 (X=4.275m to X=4.500m)	20%
	Multiple damage scenario	
DC 8	Damage at two locations of TSC1 (X=1.125m to X=1.350m) and (X=3.150m to X=3.375m)	20% 10%
DC 9	Damage at two locations of RPC 1 (X=2.025m to X=2.475m) and (X=3.150m to X=3.600m)	20% 10%
DC 10	Damage at two locations of BCSC 1 (X=0.900m to X=1.350m) and (X=3.150m to X=3.600m)	20% 10%

In single damage scenarios, 20% stiffness reduction of the cable were considered, while 10% and 20% stiffness reduction in two different locations of the cable were considered to cater for multiple damage scenarios. In real situations damage severity of cables had reached 30% [43] and therefore the damage severities (10% and 20%) considered in this study are reasonable. Moreover, the length of the damage simulated was small and ranged from 5% to 10% of the total cable length.

5.2 Damage detection without noise in modal data

Damage detection results for each damage case considered are illustrated below. Results include plots of damage indices (DI_V and DI_L) and plots of MF difference (MFD_V and MFD_L) in both damaged and undamaged cables. True damage location is indicated with red dotted lines.

5.2.1 Single Damage Scenarios

Seven damage cases were examined to study the damage locating capability of the component specific DIs and MF difference by using vertical and lateral components of mode shapes.

- Damage Case 1 (DC 1) - damage in TSC1 at mid-span

The first damage case studied is that in the middle of the TSC 1 with a 20% stiffness reduction. Numerical results of the damage indices (a) DI_V, (b) DI_L , (c) MFD_V and (d) MFD_L are shown in Fig. 8. In Fig. 8 (a), the DI_V for the damaged cable (TSC 1) reaches its maximum value at the nodes of the damaged location and no significant change can be observed in the DI_V curve for the undamaged cable (TSC 2). In Fig. 8 (b), the DI_L curves show maximum values at the damaged location in both damaged and undamaged cables and hence the results are unreliable and unable to identify the damaged cable. Similar trends can be observed in the MFD_V and MFD_L plots in Fig. 8 (c) and (d) respectively. In this damage case both DI_V and MFD_V which use the vertical components of the mode shapes, are able to detect the damage successfully at the middle of the cable, and confirm the actual location of the damage.

Further, DI_V curves plotted using the first three and first five modes for the damaged cable (TSC 1) are illustrated in Fig. 8 (e). It is evident that these two plots have very small deviations and demonstrate that the influence of higher order modes beyond mode 3 is very small. The 8.1% validation error in the fourth mode (in bridge model case 2) will therefore

not contribute much to the damage detection results. The DIs for all other damage cases were hence plotted using the first five mode shapes and natural frequencies.

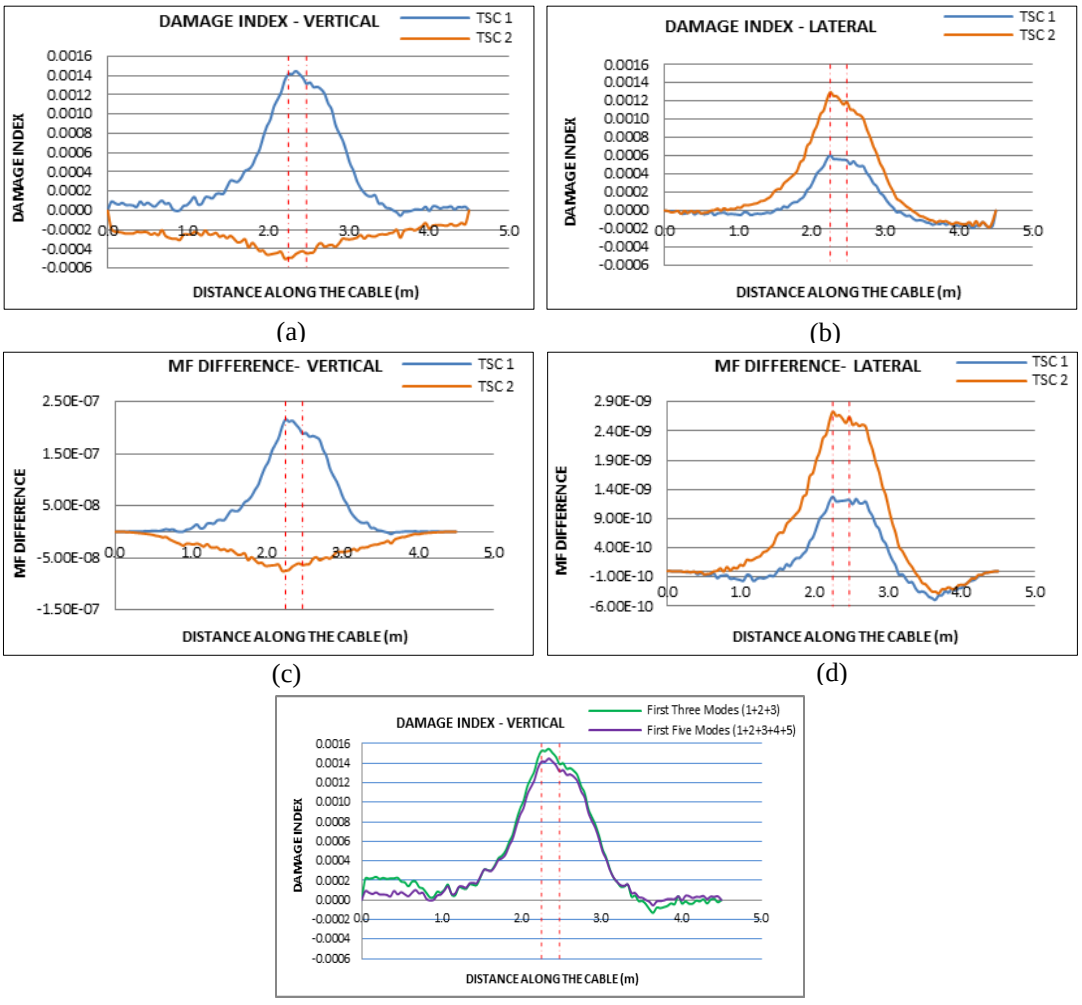


Fig. 8. DC1 - Damage indices (a) DI_V (b) DI_L and MF difference (c) MFD_V (d) MFD_L (e) DI_V curve plotted using first three and first five modes

- Damage Case 2 (DC 2) - damage in TSC1 at quarter span

Fig. 9 illustrates both the DIs and MF difference curves for the second damage case with a 20% stiffness reduction at quarter span of the TSC 1. It can be seen that the plot of DI_V peaks at the exact damage location for TSC 1 with no significant changes in the plot of DI_V for TSC 2. As also observed in the previous damage case, plots of DI_L show peaks at the damage location for both the damaged TSC 1 as well as the undamaged TSC 2. MFD_V curve peaks at damage location in TSC 1 and successfully locates the damage, while the MFD_L curves have their maximum values at the damaged location in both the damaged and undamaged cables and are hence unable to identify the damaged cable successfully. Based on the examination of the four graphs, it can be concluded that incorporating the vertical components of mode shapes for detecting damage in a suspended cable of this bridge

structure is a successful approach. The competency of DI_V and MFD_V in damage detection of cables is further evaluated through Damage Case3.

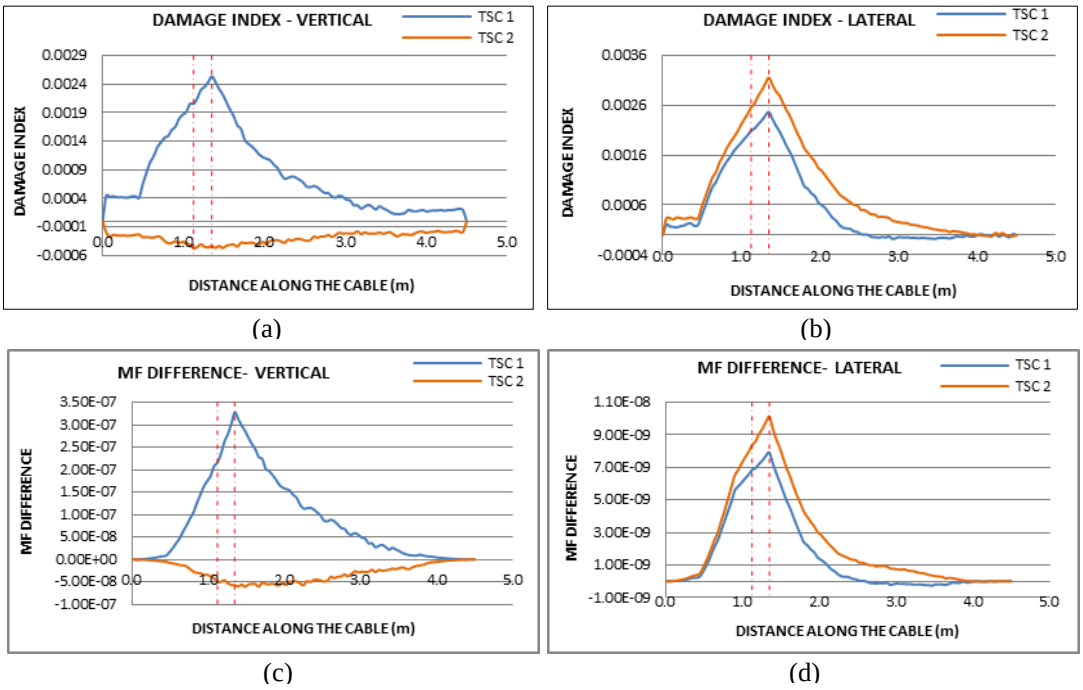


Fig. 9. DC2 - Damage indices (a) DI_V, (b) DI_L, (c) MFD_V (d) MFD_L

- Damage Case 3 (DC 3) - damage near support in TSC1

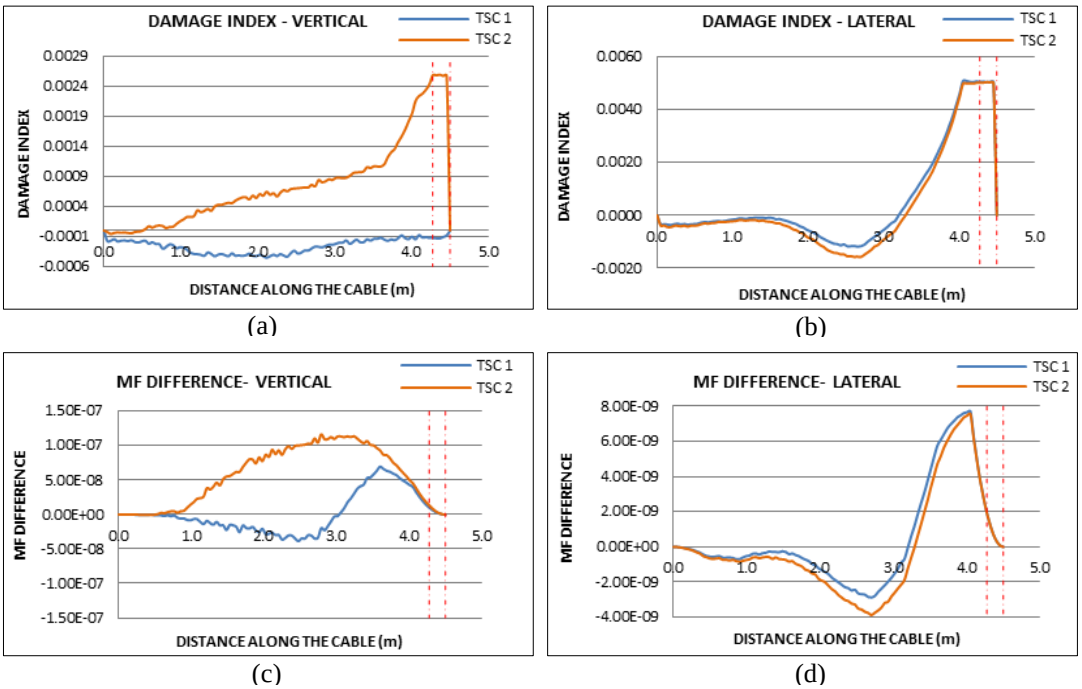


Fig. 10. DC3 - Damage indices (a) DI_V (b) DI_L and MF difference (c) MFD_V (d) MFD_L

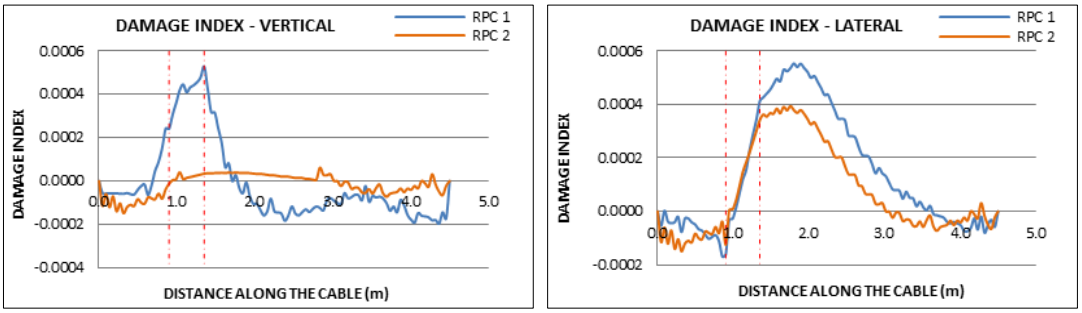
Damage Case 3 is simulated near the support in the top supporting cable 2 with 20% stiffness reduction. Results are shown in Fig. 10. As before, DI_V demonstrates a peak at the damage location in the TSC 2, while DI_L shows peaks at the damage location in both the

undamaged TSC 1 and damaged TSC 2. MFD_V and MFD_L demonstrate incorrect damage locating results. This further verifies the superior performance of DI_V compared to the other damage indices to detect damage in the TSC of a suspension bridge.

In other damage cases, similar trends were observed in the results obtained with both MFD_V and MFD_L. Hereafter, therefore, only results from DI_V and DI_L are presented for the other damage cases.

- Damage Case 4 (DC 4) - in RPC1 at quarter span

In this damage case, 20% stiffness reduction is simulated at quarter span of the pre-tensioned RPC1 (bottom). Results are shown in Fig. 11 and it can be seen that DI_V locates the damage correctly. DI_L shows peaks near the damage location in both the damaged RPC 1 and the undamaged RPC 2 and hence it is unable to locate the damage correctly. It can hence be seen that the proposed component specific DI_V incorporating the vertical components of mode shapes can successfully detect damage in the pre-tensioned reversed profile cable of a suspension bridge.

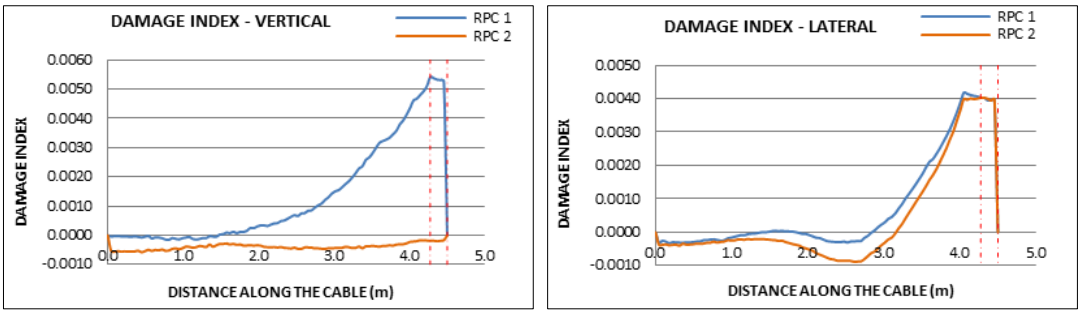


(a) (b)

Fig. 11. DC4 - Damage indices (a) DI_V (b) DI_L

- Damage Case 5 (DC 5) - damage near support in RPC1

In damage case six there is a 20% stiffness reduction near the support in the pre-tensioned RPC1. Again, DI_V demonstrates its competency in damage detection in a RPC of the suspension bridge as shown in Fig. 11. As also seen earlier, DI_L locates the damage without identifying the damaged cable.

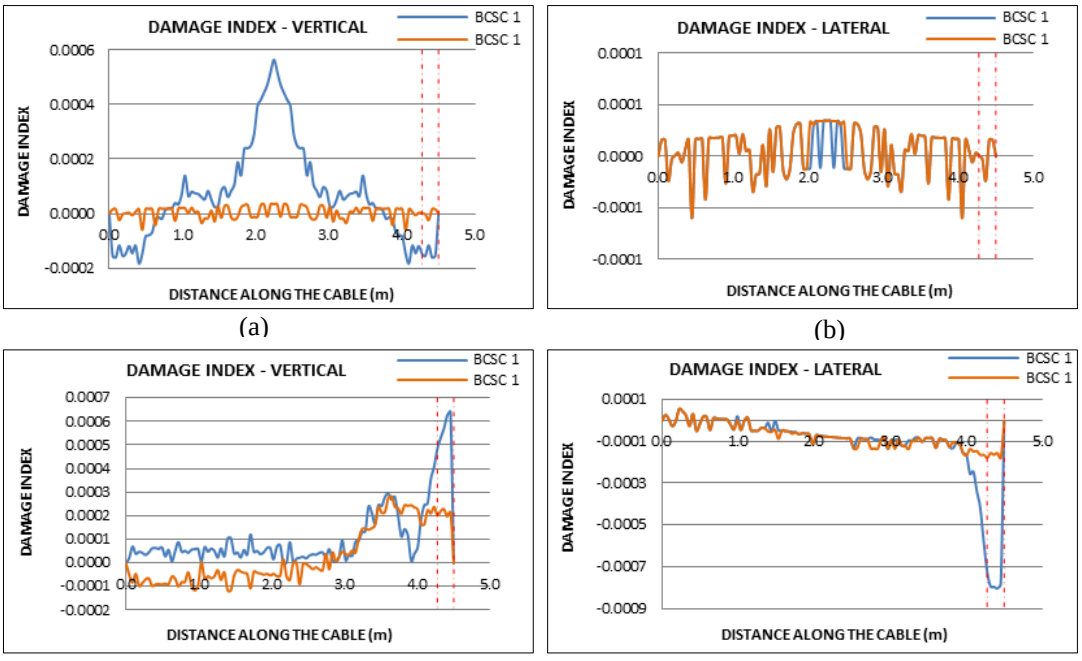


(a) (b)

Fig. 12. DC5 - Damage indices (a) DI_V (b) DI_L

- Damage Case 6 (DC 6) and Damage Case 7 (DC 7) - damage in BCSC1 at mid span and near support

The last damage cases studied under the single damage scenarios are with 20% stiffness reduction in the pre-tensioned BCSC1 in the horizontal plane at mid span and near the support. Results are shown in Fig. 13. It is evident that DI_V is able to locate the damage in the BCSC correctly in both cases while DI_L gives inconsistent results.



(a) (b)

(c) (d)

Fig. 13. DC6 - Damage indices (a) DI_V (b) DI_L and DC7 - Damage indices (c) DI_V (d) DI_L

5.2.2 Multiple Damage Scenarios

Three damage cases are examined to study the damage locating capability of component specific DIs and MF difference calculated using vertical and lateral components of mode shapes.

- Damage Case 8 (DC 8) - multiple damage in TSC1

Two locations in TSC1 are subjected to a 20% and 10% stiffness reductions in the FE model to simulate damage. Results are shown in Fig. 14 and it is clearly evident that both DI_V and MFD_V for TSC1 show two peaks corresponding to the two damage locations while DI_V and MFD_V for TSC2 have no significant variations. DI_L and MFD_L for both TSC1 and TSC2 have peaks at the damaged locations hence they give incorrect predictions.

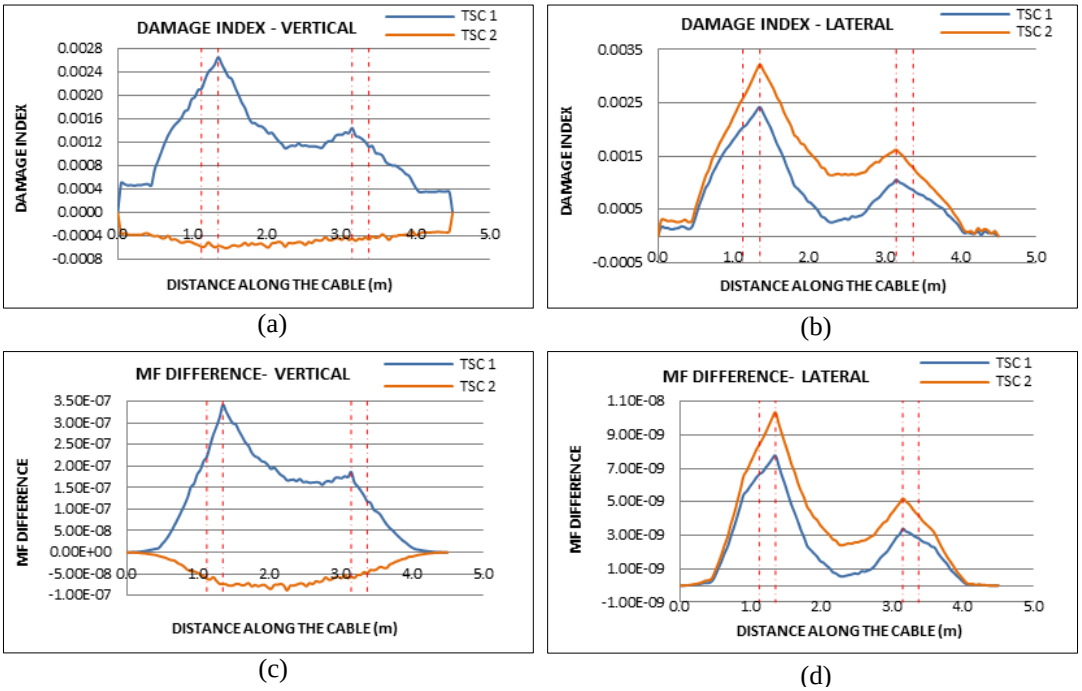


Fig. 14. DC8 - Damage indices (a) DI_V (b) DI_L, (c) MFD_V and (d) MFD_L

- Damage Case 9 (DC 9) - damage in RPC1

In this damage case, 20% and 10% stiffness reductions are simulated at mid and quarter spans of the pre-tensioned RPC1. Results are shown in Fig. 15 from which it is evident that that DI_V for RPC1 and RPC 2 has peaks at the damage locations of RPC1 while DI_L for these two cables gives inconsistent predictions.

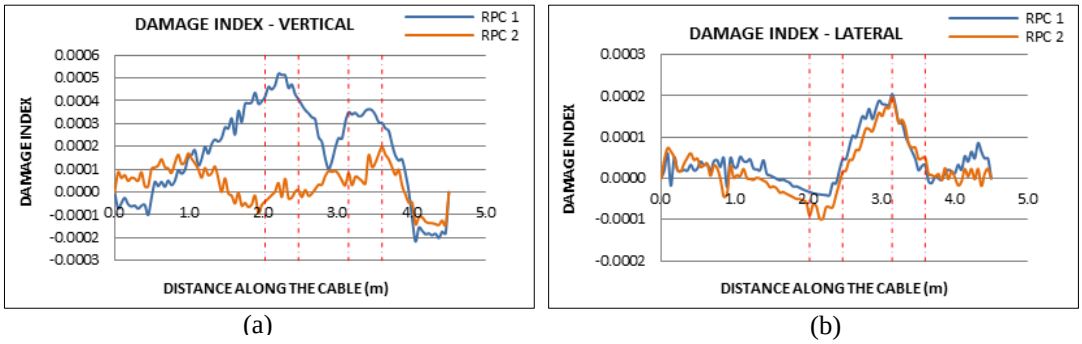
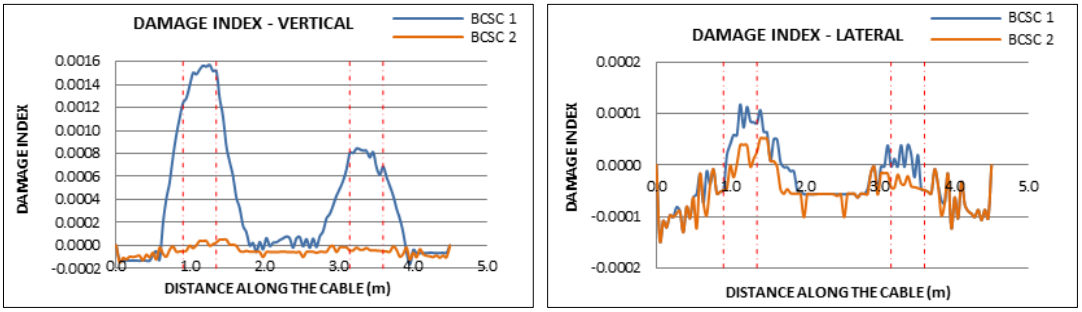


Fig. 15. DC9 - Damage indices (a) DI_V (b) DI_L

- Damage Case 10 (DC 10) - damage in BCSC`1

The last damage cases studied under the multiple damage scenarios are with 20% and 10% stiffness reductions in the pre-tensioned BCSC1 in the horizontal plane at different locations and the results are shown in Fig. 16. The results verify that DI_V is competent to detect and locate multiple damages in the pre-tensioned BCSC of a suspension bridge structure. In all further evaluations, only the damage index DI_V will be used.



(a) (b)

Fig. 16. DC10 - Damage indices (a) DI_V (b) DI_L

5.3 Damage detection with noise in modal data

In reality, measured vibration responses are associated with uncertainties such as measurement noise and computational errors in modal frequencies and mode shapes, respectively [44]. It is therefore necessary to examine the performance of the two component specific DIs in the presence of noise in the modal data. In this study, vibration responses are generated using a validated FE model and there is no noise associated with numerical simulations. As the measurement noise associated with frequencies is very low, 5% random noise is introduced to mode shapes generated from the FE model. Few selected damage cases were examined under the noisy modal data. The contaminated signal for mode shape can be represented as [45];

$$\overline{\phi_{xi}} = \phi_{xi}\left(1 + \gamma_x^{\phi}\rho_x^{\phi}\left|\phi_{max,i}\right|\right) \tag{10}$$

Where $\overline{\phi_{xi}}$ and ϕ_{xi} are mode shape components of the i^{th} mode at location x with and without noise, respectively; γ_x^{ϕ} is a random number with a mean equal to zero and a variance equals to 1; ρ_x^{ϕ} refers to the random noise level considered and $\phi_{max,i}$ is the largest component in the i^{th} mode shape.

Figs. 17 to 20 illustrate the results for locating damage using DI_V with and without noise under damage cases DC1, DC2, DC3 and DC8 respectively. The DI_V plots under noisy modal data, for the damage cases considered have similar features as observed earlier for

noise free condition. They have clear peaks at the damage locations in both single and multiple damage cases. This shows that DI_V using the vertical components of the vibration modes performs well for locating damage even in the presence of 5% noise in the mode shape data.

The results in this section confirm that the proposed component specific DI_V is capable of detecting and locating damage in all three types of cables in the suspension bridge structure.

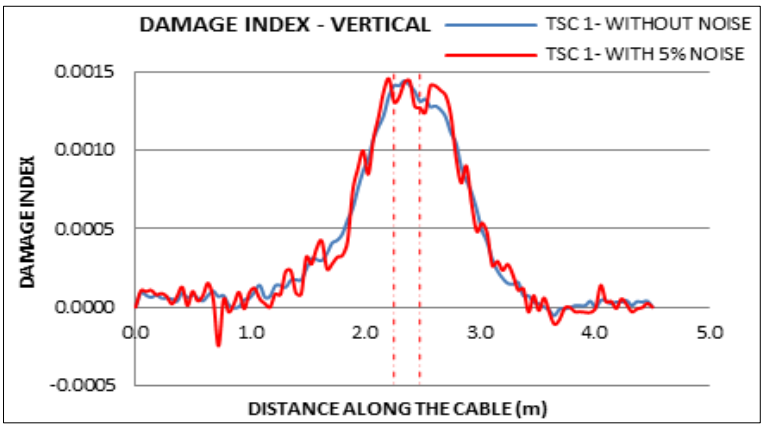


Fig. 17. DC1 - DI_V

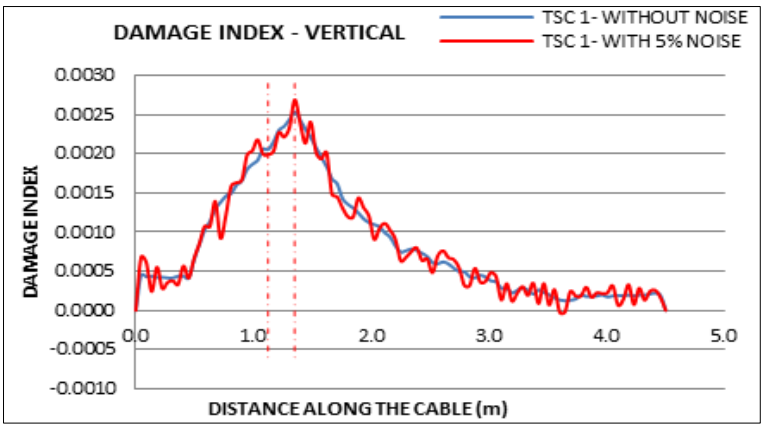


Fig. 18. DC2 - DI_V

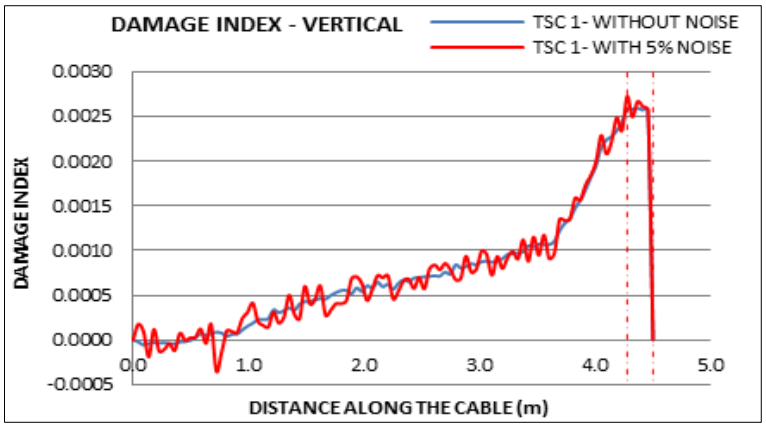


Fig. 19. DC3 - DI_V

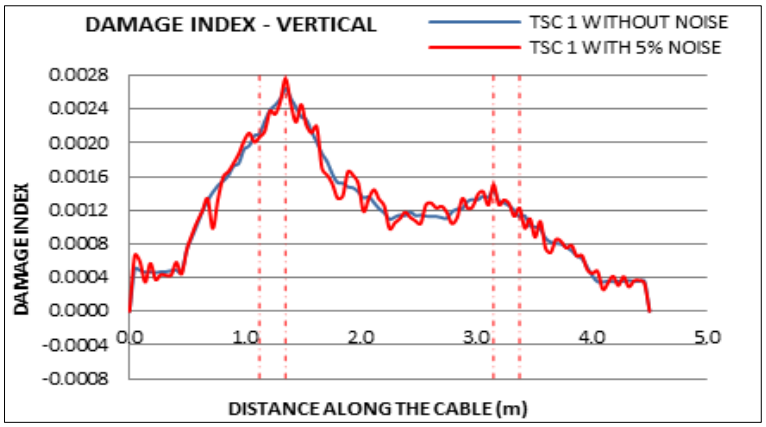
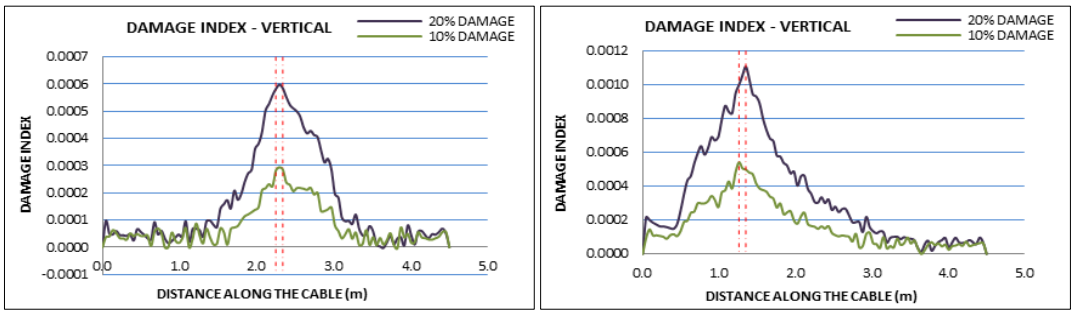


Fig. 20. DC8 - DI_V

5.4 Further Evaluation of Vertical Damage Index (DI_V)

Suspension bridge cables are encased in cable protection systems and damage due to corrosion in them are not visible during bridge inspection until the damage become more severe. Therefore, in the previous sections, performance of the proposed DI_V was evaluated for a small damage severity of (20%) across the length of the cable ranging from 5% to 10% of its total length. In this section, the effectiveness of DI_V is evaluated for much smaller damaged lengths of cables. Two damage cases with 20% and 10% stiffness reductions at mid span and quarter span were considered in the TSC1 across 0.09m which is 2% of the total cable length. Fig. 21 illustrates the performance of DI_V and it is evident that in both cases, damage was detected successfully. The DI_V was further evaluated for both damage severities at mid span of the same cable, but across a smaller damage length of 1%. Fig. 22 illustrates the damage detection results. The DI_V curves corresponding to both damage severities predict the damage zone reasonably well, even though the peaks are somewhat indistinct. These results show that even though the efficiency of the proposed damage index DI_V seems to

reduce with a reduction in the damage length, useful results can be obtained even when the damage length is as small as 1% of the total cable length.



(a) (b)

Fig. 21. Damage detection in TSC1 with 0.09m (2%) damage length with 10% and 20% stiffness reductions (b) Damage at mid span (b) Damage at quarter span

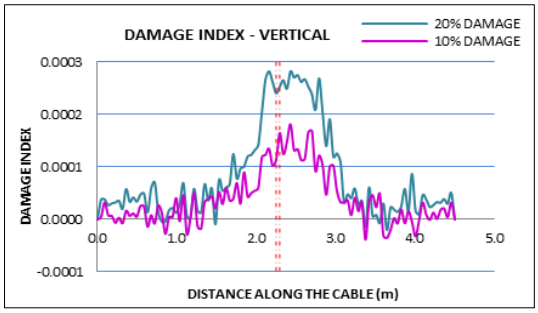
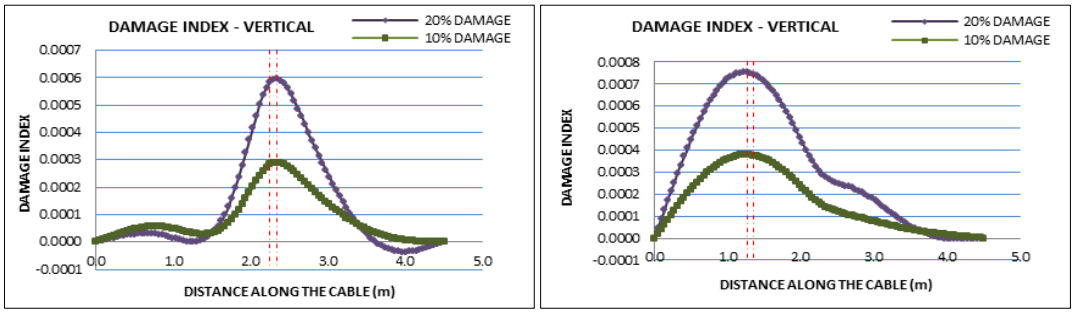


Fig. 22. Damage detection in TSC1 with 0.045m (1%) damage length with 10% and 20% stiffness reductions

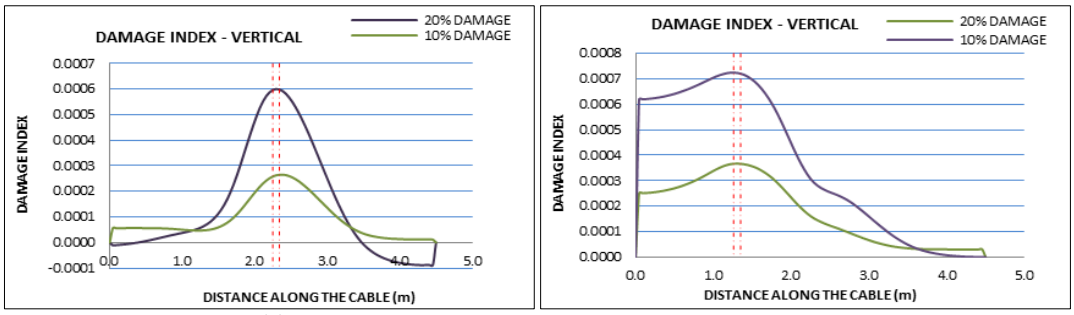
Further evaluation of DI_V was carried out to test its capability when modal data can only be obtained from a limited no of sensors. As it was not possible to damage the physical model of the bridge, this study was conducted using simulations. Two damage severities of 20% and 10% (i) at mid span and (ii) at quarter span of the TSC1 across a cable length of 0.09m (2% of total cable length) were considered. For this case, the mode shape data from the simulations was obtained only at the locations corresponding to the 5 sensor locations (Fig. 4) used in the experiments. To deal with this problem (under these circumstances), some form of data interpolation would need to be used and this paper presents two ways to do this. In the first approach, 5 DI_V data points were calculated (directly from 5 mode shape data points) and then fitted with the cubic spline interpolation to produce the (complete) DI_V curve as reported in Figure 23. In the second way, cubic spline interpolation was first applied on 5 mode shape data points to expand it into a (complete) mode shape dataset before this dataset was used to calculate the DI_V curve as plotted in Figure 24. Note that the second method was also known as mode shape reconstruction using cubic spline interpolation (see for example [46]) which simply means reconstructing the full mode shape curve from a limited number of

measured mode shape data points. It is evident that the results in the two figures are in excellent agreement and this once again reconfirms the robustness of DI_V index.



(a) (b)

Fig. 23. DI calculated with limited sensors and fitted with cubic spline (a) Damage at mid span (b) Damage at quarter span



(a) (b)

Fig. 24. DI calculated with reconstructed mode shapes fitted with cubic spline (a) Damage at mid span (b) Damage at quarter span

6 Conclusion

Suspension bridges play an important role in the transport network of a city. These are large structure and damage in them can go unnoticed during their long service lives. It is therefore necessary to develop a method to detect damage at an early stage in these structures so that appropriate retrofitting can be carried out to prevent bridge failure.

Though vibration based methods have been used in detecting damage in some structures, they pose some difficulties with suspension bridges. These bridges are slender structures which exhibit complex vibration modes which are difficult to capture and use with the VBDD methods. This paper proposes a mode shape component specific damage index (DI) that can successfully detect and locate damage in the main cables and of a suspension bridge. This DI incorporates only a few lower order modes and is a variation of the traditional MF method. It's effectiveness to detect and locate damage in the cables of a suspension bridge is demonstrated through a number of illustrations.

A laboratory model of a suspension bridge with pre-tension cables was selected to test the damage detection process. This bridge model had top supporting cables, bottom pre-tensioned reverse profile cables in the vertical plane and pre-tensioned bi-concave side cables in the horizontal plane. Since vertical and torsional vibration modes were present in the first few vibration modes, components specific DIs (DI_L and DI_V) which incorporate only the lateral and vertical components of the mode shapes respectively were developed and applied to detect and locate damage in the three different types of the cables under single and multiple damage scenarios. It has been shown that the vertical damage index calculated using only the vertical components of the mode shapes (DI_V) can detect and locate damage successfully in all three types of cables under both single and multiple damage scenarios. The main findings of this study are presented below:

- Results obtained with the proposed DI_V showed its superior damage detection capability compared with the traditional MF difference method.
- The proposed DI_V was capable of successfully detecting damage in all three cable types; the top supporting, bottom reverse profiled and bi-concave side cables, under all damage scenarios considered. Damage severities of 10%-20% stiffness reductions across 1% - 10% cable lengths were treated.
- It was shown that DI_V can successfully detect and locate damage even in the presence of 5% measurement noise in mode shape data for the all damage scenarios considered.
- Damage detection capability of DI_V with limited modal data was also shown. It was evident that DI_V can accurately detect damage with 10% to 20% of stiffness reductions across 2% of cable length, when modal data from a limited number of locations is used.
- The contribution of higher order modes to the damage detection ability of the proposed DI was small and reasonably accurate damage detection results can be obtained using only the first three modes of vibration (with the proposed DI).
- Due to the higher modal mass distribution in the vertical direction of this bridge, DI_V showed better performance in damage detection. This is also evidenced by the fact that the dominant vibration in this suspension bridge model was in the vertical direction, and therefore, DI_V showed better performance in damage detection in the cables of this suspension bridge.

Overall, the applicability of a component specific DI for detecting and locating damage in the different cables of this rather complex suspension bridge structure with pre-tensioned cables has been demonstrated. The findings of this study can be used to detect damage in the main cables of suspension bridges to enhance their life spans.

7 Acknowledgments

This research forms a part of a study of structural health monitoring of structures at Queensland University of Technology, Australia. Wasanthi R. Wickramasinghe is a PhD student supported by Queensland university of Technology Postgraduate Research Award. The guidance provided by the supervisors is greatly appreciated. Further, facilities provided to conduct the experiment by Banyo Pilot Plant Precinct and Engineering Precinct of QUT are also acknowledged.

8 References

[1] H.W. Shih, D. Thambiratnam, T.H.T. Chan, Damage detection in truss bridges using vibration based multi-criteria approach, Structural Engineering and Mechanics, 39 (2011) 187-206.
[2] T.M. Whalen, The behavior of higher order mode shape derivatives in damaged, beam-like structures, Journal of sound and vibration, 309 (2008) 426-464.
[3] B.L. Wahalathantri, D.P. Thambiratnam, T.H. Chan, S. Fawzia, Vibration based baseline updating method to localize crack formation and propagation in reinforced concrete members, Journal of Sound and Vibration, 344 (2015) 258-276.
[4] A. Alvandi, C. Cremona, Assessment of vibration-based damage identification techniques, Journal of Sound and Vibration, 292 (2006) 179-202.
[5] F.L. Wang, T.H. Chan, D.P. Thambiratnam, A.C. Tan, C.J. Cowled, Correlation-based damage detection for complicated truss bridges using multi-layer genetic algorithm, Advances in Structural Engineering, 15 (2012) 693-706.
[6] Y. Yan, H. Hao, L. Yam, Vibration-based construction and extraction of structural damage feature index, International journal of solids and structures, 41 (2004) 6661-6676.
[7] F. Choi, J. Li, B. Samali, K. Crews, Application of the modified damage index method to timber beams, Engineering Structures, 30 (2008) 1124-1145.
[8] J.T. Kim, J.H. Park, B.J. Lee, Vibration-based damage monitoring in model plate-girder bridges under uncertain temperature conditions, Engineering Structures, 29 (2007) 1354-1365.
[9] Y. Zhang, L. Wang, S.T. Lie, Z. Xiang, Damage detection in plates structures based on frequency shift surface curvature, Journal of Sound and Vibration, 332 (2013) 6665-6684.
[10] H.A. Razak, F. Choi, The effect of corrosion on the natural frequency and modal damping of reinforced concrete beams, Engineering Structures, 23 (2001) 1126-1133.
[11] R. Curadelli, J. Riera, D. Ambrosini, M. Amani, Damage detection by means of structural damping identification, Engineering Structures, 30 (2008) 3497-3504.
[12] R.J. Allemang, The modal assurance criterion–twenty years of use and abuse, Sound and vibration, 37 (2003) 14-23.
[13] S. Choi, S. Park, N. Stubbs, Nondestructive damage detection in structures using changes in compliance, International Journal of Solids and Structures, 42 (2005) 4494-4513.
[14] V. Dawari, G. Vesmawala, Modal Curvature and Modal Flexibility Methods for Honeycomb Damage Identification in Reinforced Concrete Beams, Procedia Engineering, 51 (2013) 119-124.

[15] M. Cao, M. Radzieński, W. Xu, W. Ostachowicz, Identification of multiple damage in beams based on robust curvature mode shapes, Mechanical Systems and Signal Processing, 46 (2014) 468-480.
[16] A.K. Pandey, M. Biswas, Damage detection in structures using changes in flexibility, Journal of Sound and Vibration, 169 (1994) 3-17.
[17] T. Toksoy, A. Aktan, Bridge-condition assessment by modal flexibility, Experimental Mechanics, 34 (1994) 271-278.
[18] A. Pandey, M. Biswas, Experimental verification of flexibility difference method for locating damage in structures, Journal of Sound and Vibration, 184 (1995) 311-328.
[19] J.Y. Wang, J.M. Ko, Y.Q. Ni, Modal sensitivity analysis of Tsing Ma Bridge for structural damage detection, in: SPIE's 5th Annual International Symposium on Nondestructive Evaluation and Health Monitoring of Aging Infrastructure, International Society for Optics and Photonics, 2000, pp. 300-311.
[20] Y. Ni, H. Zhou, K. Chan, J. Ko, Modal Flexibility Analysis of Cable-Stayed Ting Kau Bridge for Damage Identification, Computer-Aided Civil and Infrastructure Engineering, 23 (2008) 223-236.
[21] P.H.N. Moragaspitiya, D.P. Thambiratnam, N.J. Perera, T.H.T. Chan, Development of a vibration based method to update axial shortening of vertical load bearing elements in reinforced concrete buildings, Engineering Structures, 46 (2013) 49-61.
[22] M. Montazer, S. Seyedpoor, A New Flexibility Based Damage Index for Damage Detection of Truss Structures, Shock and Vibration, 2014 (2014).
[23] S. Sung, K. Koo, H. Jung, Modal flexibility-based damage detection of cantilever beam-type structures using baseline modification, Journal of Sound and Vibration, (2014).
[24] N. Stubbs, J. Kim, K. Topole, An efficient and robust algorithm for damage localization in offshore platforms, in: Proc. ASCE Tenth Structures Congress, 1992.
[25] P. Cornwell, S.W. Doebling, C.R. Farrar, Application of the strain energy damage detection method to plate-like structures, Journal of Sound and Vibration, 224 (1999) 359-374.
[26] H.W. Shih, D. Thambiratnam, T.H.T. Chan, Vibration based structural damage detection in flexural members using multi-criteria approach, Journal of Sound and Vibration, 323 (2009) 645-661.
[27] E. Manoach, I. Trendafilova, Large amplitude vibrations and damage detection of rectangular plates, Journal of Sound and Vibration, 315 (2008) 591-606.
[28] C.R. Farrar, D.A. Jauregui, Comparative study of damage identification algorithms applied to a bridge: I. Experiment, Smart Materials and Structures, 7 (1998) 704.
[29] W.R. Wickramasinghe, Damage detection in suspension bridges using vibration characteristics in: School of Civil Engineering & Built Environment, Queensland University of Technology (QUT), , 2015.
[30] S.W. Doebling, C.R. Farrar, Computation of structural flexibility for bridge health monitoring using ambient modal data, in: Proceedings of the 11th ASCE Engineering Mechanics Conference, Citeseer, 1996, pp. 1114-1117.
[31] Y. Gao, B. Spencer, Damage localization under ambient vibration using changes in flexibility, Earthquake Engineering and Engineering Vibration, 1 (2002) 136-144.
[32] E. Parloo, B. Cauberghe, F. Benedettini, R. Alaggio, P. Guillaume, Sensitivity-based operational mode shape normalisation: application to a bridge, Mechanical Systems and Signal Processing, 19 (2005) 43-55.
[33] A. Yan, J.-C. Golinval, Structural damage localization by combining flexibility and stiffness methods, Engineering Structures, 27 (2005) 1752-1761.
[34] M.H. Huang, D.P. Thambiratnam, N.J. Perera, Vibration characteristics of shallow suspension bridge with pre-tensioned cables, Engineering structures, 27 (2005) 1220-1233.
[35] H. Li, H. Yang, S.-L.J. Hu, Modal strain energy decomposition method for damage localization in 3D frame structures, Journal of engineering mechanics, 132 (2006) 941-951.
[36] C. Rainieri, G. Fabbrocino, Operational Modal Analysis of Civil Engineering Structures: An Introduction and Guide for Applications, Springer, 2014.

[37] A. Cunha, E. Caetano, F. Magalhães, Output-only dynamic testing of bridges and special structures, Structural Concrete, 8 (2007) 67-85.
[38] R. Brincker, P. Andersen, R. Cantieni, Identification and level I damage detection of the Z24 highway bridge, Experimental techniques, 25 (2001) 51-57.
[39] L. Zhang, R. Brincker, P. Andersen, An overview of operational modal analysis: major development and issues, Mechanical Systems and Signal Processing, (2009).
[40] T. Nguyen, T.H. Chan, D.P. Thambiratnam, Effects of wireless sensor network uncertainties on output-only modal analysis employing merged data of multiple tests, Advances in Structural Engineering, 17 (2014) 319-330.
[41] R. Cantieni, Experimental methods used in system identification of civil engineering structures, in: Proceedings of the International Operational Modal Analysis Conference (IOMAC), 2005, pp. 249-260.
[42] P. ANSYS Inc.(Canonsburg, 2012), Version 14.5, in: Workbench, ANSYS.
[43] M.J.D. Sloane, R. Betti, G. Marconi, A.L. Hong, D. Khazem, An Experimental Analysis of a Non-Destructive Corrosion Monitoring System for Main Cables of Suspension Bridges, Journal of Bridge Engineering, (2012).
[44] Z. Shi, S. Law, L. Zhang, Damage localization by directly using incomplete mode shapes, Journal of Engineering Mechanics, 126 (2000) 656-660.
[45] Z. Shi, S. Law, L.M. Zhang, Structural damage detection from modal strain energy change, Journal of engineering mechanics, 126 (2000) 1216-1223.
[46] A.A. Cury, C.C.H. Borges, F.S. Barbosa, A two-step technique for damage assessment using numerical and experimental vibration data, International journal of structural health monitoring, 10 (4) 417-428.